LA-UR -91-1648

LA-UR--91-1648

DE91 013031

Los Alamos National Laboratory is operated by the University of California for the United States Department of Energy under contract W-7405-ENG-36

TITLE DYNAMIC PLASTICITY IN TRANSITION FROM THERMAL ACTIVATION TO VISCOUS DRAG

AUTHOR(S) J. N. Johnson and D. L. Tonks

SUBMITTED TO 1991 APS Topical Conference on the Shock Compression of Condensed Matter
June 17-20, 1991, Williamsburg, Virginia

DISCLAIMER

Los Alamos National Laboratory
Los Alamos, New Mexico 87545

DYNAMIC PLASTICITY IN TRANSITION FROM THERMAL ACTIVATION TO VISCOUS DRAG

J. N. JOHNSON and D. L. TONKS

Theoretical Division, Los Alamos National Laboratory, Los Alamos, NM 87545

For low-to-intermediate rates of mechanical loading, plastic deformation is controlled by thermal activation or mechanical penetration of dislocations through barriers. These barriers can be solute atoms, impurities, or, in the case of very pure materials, other dislocations. At some point between intermediate strain rates ($10 - 10^4$ s^{-1}) and the higher strain rates ($10^6 - 10^7$ s^{-1}) associated with weak-shock compression, the plastic deformation process makes a transition from being dominated by stress-assisted thermal activation to being controlled by the time it takes a mobile dislocation to get from one barrier to the next: this latter time depends on the effective stress and viscous-drag force provided by the perfect lattice. Some of the models that describe this process are reviewed, along with various hardening mechanisms. Distinction is made between simple rate-dependent models (in which the shear stress depends on the current plastic strain rate and plastic strain) and path-dependent models (in which the shear stress depends on the current plastic strain rate and all past history through one, or more, internal-state variables). A way in which shock-wave data can be used to extend intermediate strain-rate models into the viscous-drag regime is described.

1. INTRODUCTION

A major challange to shock compression scientists has been the inference of dynamic mechanical properties from limited "real-time" gauge records, shock-recovery experiments, low-to-intermediate strain-rate data, and reasonable, physically based micromechanical models. The cyclic process of experiment/theory has been going on ever since Pack, Evans, and James[1] obtained the first indirect evidence of an elastic precursor in explosively loaded steel. Of course, materials scientists have been measuring and modeling low-to-intermediate strain-rate behavior for some time. It is only lately that we have begun to merge these two regimes. Recent discussions regarding intermediate strain-rate data (particularly for copper) have focused on an increase in strain-rate sensitivity for strain rates above 10^3 s^{-1}: initial explanations were based on a change in deformation mechanism from thermal activation to dislocation drag.[2-5]

Further experimentation and interpretation have suggested that some part, or all, of the increase in strain-rate sensitivity for OFE copper is due to rate-dependent hardening of the mechanical threshold stress,[6] at least to a maximum strain rate of approximately 2×10^4 s^{-1}. The mechanical threshold stress (abbreviated MTS here) is defined to be the yield strength at 0 K. Tonks and Johnson[7] examined shock-wave data for copper in terms of the MTS model, and concluded that the dislocation-drag regime was reached for shock amplitudes of 3.0- and 5.4-GPa. The scope of the present paper is (i) to review models that combine thermal activation and dislocation drag, (ii) to assess them in terms of current experimental data in both the low-to-intermediate (10^{-4} - 10^4 s^{-1}) and plate-impact (10^5 - 10^7 s^{-1}) strain-rate regimes, and (iii) to present an estimate of where the transition between the two deformation mechanisms occurs for OFE copper.

2. MODELS AND HARDENING MECHANISMS

2.1. Clifton

Clifton[2] gives the earliest and most complete discussion of transition from thermal activation to dislocation drag in shock-loaded solids, with specific application to 6061-T6 aluminum. The plastic strain rate $\dot{\epsilon}^P$ is related to the magnitude of the Burgers vector b, the mobile dislocation density N_m, and the average dislocation velocity $\bar{v}$ according to the Orowan relation:

$$\dot{\epsilon}^P = b\, N_m\, \bar{v} \quad . \tag{1}$$

The motion of dislocations due to an applied stress τ is viewed as being composed of thermal activation through disperse local obstacles and viscous glide through the clear region between obstacles of spacing L. Hence

$$\bar{v} = L/(t_1 + t_2) \quad , \tag{2}$$

where t_1 is the time for thermal activation and t_2 is the time for traveling to the next obstacle:

$$t_1 = \nu_0^{-1}(\exp[\Delta G(\tau)/kT] - 1) \quad , \tag{3}$$

$$t_2 = L/v(\tau) \quad , \tag{4}$$

where

$$\Delta G(\tau) = \Delta G_0(1 - [(\tau - \tau_a)/\tau_p]^{2/3})^{3/2} \tag{5}$$

is the difference between the Gibbs free energies at adjacent stable and metastable equilibrium positions, τ_a is the magnitude of the long-range residual stress, τ_p is the peak stress required to mechanically overcome the obstacle, T is the absolute temperature, and $v(\tau)$ is the dislocation velocity due to viscous drag in the clear region between obstacles. The terms ν_0 and ΔG_0 represent an attempt frequency and peak activation energy, respectively. The -1 term in Equation (3) is introduced to ensure that $t_1=0$ at $\tau=\tau_a+\tau_p$; in regions for which ΔG is sufficiently large, Equation (3) reduces to the usual expression for thermal activation. Generally $v(\tau)$ is taken to be of the form

$$v(\tau) = b\tau/B \quad , \tag{6}$$

where B is the drag coefficient, which becomes infinitely large as v approaches c_s, the elastic shear wave speed; this has the effect of limiting v to the region between zero and c_s. Combination of Equations (2)-(5) then leads to the following expression for $\bar{v}$ in the transition region:

$$\bar{v} = L\nu_0(\exp[\Delta G(\tau)/kT] - 1 + L\nu_0/v(\tau))^{-1} \quad . \tag{7}$$

The behavior of $\bar{v}/c_s$ as a function of τ is shown in Figure 1. The plastic strain rate is then obtained from $\bar{v}$ and Equation (1) with some assumptions concerning the mobile dislocation density N_m as a function of the plastic strain.

The major thrust of this work involves shock-wave response, not intermediate strain-rates in the thermal activation regime, and hence details of where the transtion region is located are not investigated. A significant conclusion of this work is that the approximately linear relationship for dislocation velocity, Equation (6), cannot successfully predict the dispersive nature of wave profiles at low impact velocities while also predicting fast rising shocks and approximately steady waves at 1 mm from the impact surface in 6061-T6 aluminum for symmetric impact velocities on the order of 0.5 km/s.

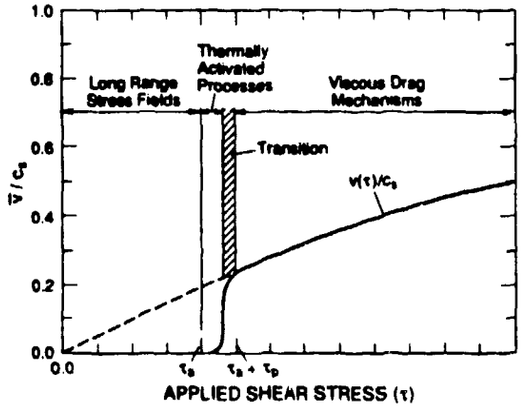

FIGURE 1
Transition to dislocation drag

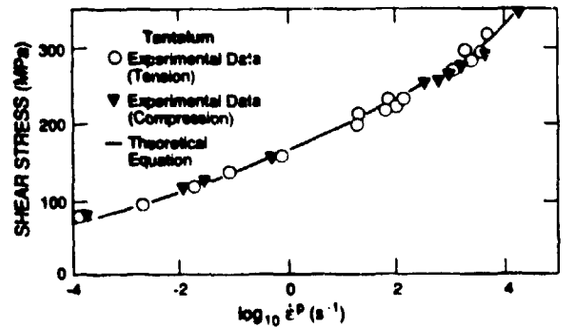

FIGURE 2
Theory and data for tantalum

2.2. Hoge and Muhkerjee

Experimental data on tantalum at strain-rates of 10^{-4} to 10^{4} s^{-1} have been analyzed by Hoge and Muhkerjee[3] in terms of thermal activation in combination with transition to dislocation drag. Their expression for the average dislocation velocity is

$$\bar{v} = L\nu_0[\exp[\Delta G(\tau)/kT] + L\nu_0 B_0/2\tau' b]^{-1}, \qquad (8)$$

where the activation energy is of the form

$$\Delta G(\tau) = 2U_k[1 - (\tau'/\tau_p)]^2 \quad . \qquad (9)$$

In Equations (8) and (9) τ' is the thermal component of the stress (the difference between the measured flow stress τ and the athermal, long-range, internal back stress τ_a) and τ_p is the Peierls stress. The similarities to the expressions of Clifton[2] and Follansbee, Regazzoni, and Kocks[4] are apparent. The comparison of this model with experimental data on tantalum is shown in Figure 2. The transition from thermal activation to dislocation drag is gradual and takes place at a strain rate of approximately 10^{3} s^{-1}.

Steinberg and Lund[8] have applied the results of Hoge and Muhkerjee to a computer algorithm for simulation of shock compression in tantalum. In this work τ and τ' are interpreted as yield strengths, and $\dot{\epsilon}^p$ in Equation (1) is taken to be the total strain rate rather than the plastic strain rate. Therefore, comparison to standard, physically based interpretations is difficult.

2.3. Follansbee, Regazzoni, and Kocks

Follansbee, Regazzoni, and Kocks[4] follow a method very similar to that of Clifton[2] in describing the the dramatic increase in strain-rate sensitivity for strain rates exceeding 10^{3} s^{-1} in copper. The strain-rate dependence of the flow stress in copper at a strain of 15 percent is shown in Figure 3.

In this model, the energy for thermal activation is expressed in terms of the "threshold stress" τ_a, the flow stress at 0 K. The measurement of τ_a in this work was done at a strain rate of 5500 s^{-1} and so strictly applies to the internal (metallurgical) structure produced at this strain rate. It is assumed that the plastic strain constitutes an

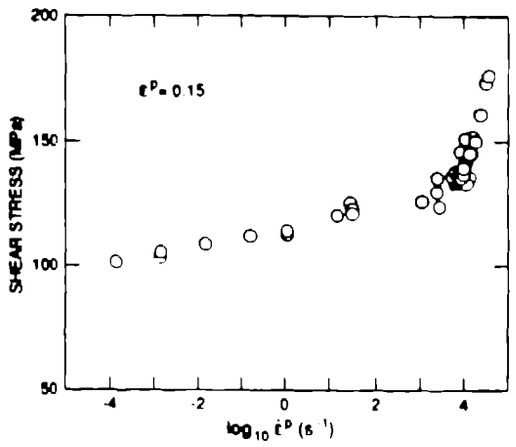

FIGURE 3
Shear stress data for OFE copper (ref. 4)

approximate representation of the internal structure. The Gibbs free energy of thermal activation is assumed to be given by

$$\Delta G(\tau) = F_0[1 - (\tau/\tau_a)^{1/2}]^{3/2} , \qquad (10)$$

where F_0 is a constant = 220 kT. The average dislocation velocity is given by

$$\bar{v} = L\omega_0[\exp[\Delta G(\tau)/kT] + L\omega_0 M B_0/(2\tau b)]^{-1}, \quad (11)$$

where M is an average Taylor factor and other quantities have already been defined. We note the similarities with Clifton's[2] results, Equations (5)-(7): the quantity B_0 represents the drag coefficient in the limit of low dislocation velocities and low applied stresses [throughout this work we make the distinction between uniaxial stress σ and shear stress τ; $\sigma = 2\tau$].

Equation (11) goes smoothly over to the dislocation drag regime as $\Delta G \to 0$. A limitation of this analysis is that $\tau \leq \tau_a$ because of the mathematical form of Equation (10). Various assumptions are made concerning the mobile dislocation density, and the model is compared with the experimental data as shown in Figure 4 with $N_a = N_{a0}(\tau/\tau_a)^n$; n = 2 (solid line) and n = 3 (dashed line). The transition from thermal activation to dislocation drag is indicated by the arrow (Figure 4). Additional experimentation reveals that

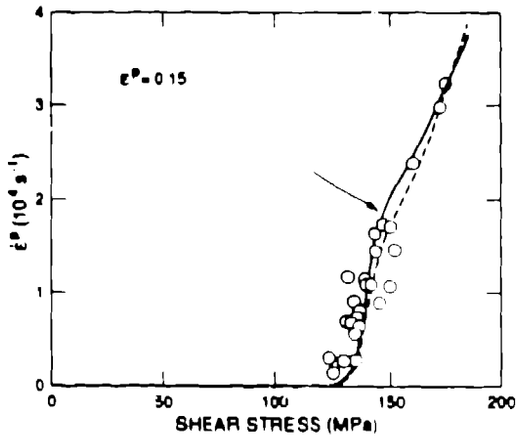

FIGURE 4
Theory and data for OFE copper (ref. 4)

the assumption regarding the independence of τ_a on plastic strain rate is in error, and the data are reexamined in the work of Follansbee and Kocks.[6]

2.4. Armstrong and Zerilli

Armstrong and Zerilli[5] have also investigated the transition to dislocation drag in copper. The empirical relationships include strain hardening, strain-rate affects, and thermal softening. An approximate description of the complete process of transition to dislocation drag is given by a drag-affected, additive thermal stress

$$\tau^* = (1/4)\sigma_{th}[1 + (1 + 4c_0/\dot{\varepsilon}^p T/\sigma_{th})^{1/2}] , \qquad (12)$$

where

$$\sigma_{th} = B_1(\epsilon^p)^{1/2} \exp[(-\beta_0 + \beta_1 \ln \dot{\epsilon}^p)T] \quad , \quad (13)$$

and c_0, B_1, β_0, and β_1 are empirical constants. Figure 5 shows a fit of the Armstrong-Zerilli model to the data of Follansbee, Regazzoni, and Kocks.[4]

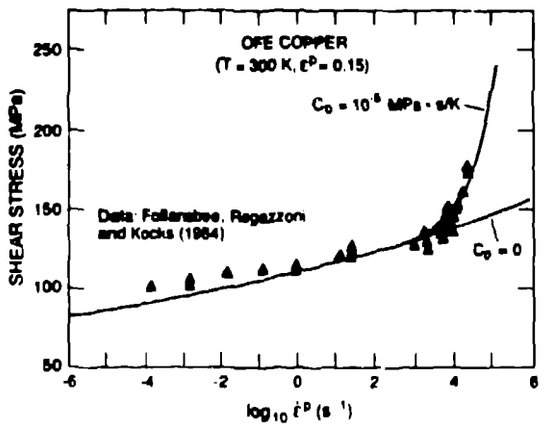

FIGURE 5
Theory and data for OFE copper (ref. 5)

2.5. Follansbee and Kocks (MTS)

In the recent work of Follansbee and Kocks[6] a new explanation for the increased strain-rate sensitivity of OFE copper at a strain rate of 10^3 s^{-1} is put forth. This work follows from that of Follansbee, Regazzoni, and Kocks[4] and involves additional measurement of the reload strength of samples that have been prestrained to the same final strain but at vastly different rates. The data show that the threshold stress, now termed the mechanical threshold stress (MTS), undergoes a dramatic increase in hardening rate ($d\tau_a/d\epsilon^p$) for strain rates exceeding 10^3 s^{-1}. The essence of these measurements and their interpretation are shown in Figure 6 in which two identical samples are prestrained to 15 percent at strain rates of 10^4 s^{-1} and 10^{-4} s^{-1} and then reloaded at the same (10^{-3} s^{-1}) strain rate. The difference in yield strength for these two tests shows the difference in internal structure produced by the two prestrain conditions; that is, the material has a memory of its past history and the increase in strain-rate sensitivity shown in Figure 3 is a result of internal structural evolution and has nothing to do with transition to dislocation drag.

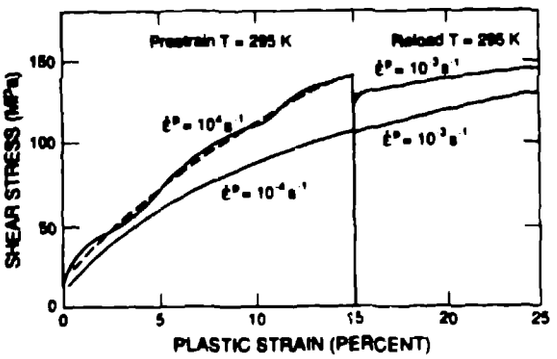

FIGURE 6
Reload tests on OFE copper

In the MTS model the plastic strain rate in the absence of dislocation drag is given by (thermal activation only)

$$\dot{\epsilon}_i^p = \nu_0 \exp[-\Delta G(\tau)/kT] \quad , \quad (14)$$

where

$$\Delta G(\tau) = 1.6\mu b^3\left(1 - [(\tau-\tau_a)/(\tau_s-\tau_a)]^{2/3}\right), \quad (15)$$

μ is the temperature dependent shear modulus, $\nu_0 = 10^7$ s^{-1}, and $\tau_a = 20$ MPa. The evolution of the MTS is assumed to be of the form

$$d\tau_s/d\epsilon^p = \theta_0\left(1 - \frac{\tanh[(\tau_s - \tau_a)/(\tau_s - \tau_a)]}{\tanh(2)}\right) \quad , \quad (16)$$

where τ_s is a saturation stress (a function of strain rate and temperature).

When all of the data have been fit according to these assumptions, $\theta_0(\dot{\epsilon}^p)$ varies as shown in Figure 7 (circles) along with an

empirical fit (solid line) as given by

$$\theta_0(\text{kbar}) = (1/2)[23.90 + 0.12 \ln \dot{\epsilon}^P(s^{-1}) + 3.4 \times 10^{-4} \dot{\epsilon}^P(s^{-1})] \quad . \tag{17}$$

These results do not mean that transition to dislocation drag does not occur at some point, only that previous interpretations of the data shown in Figure 3 are due to other factors.

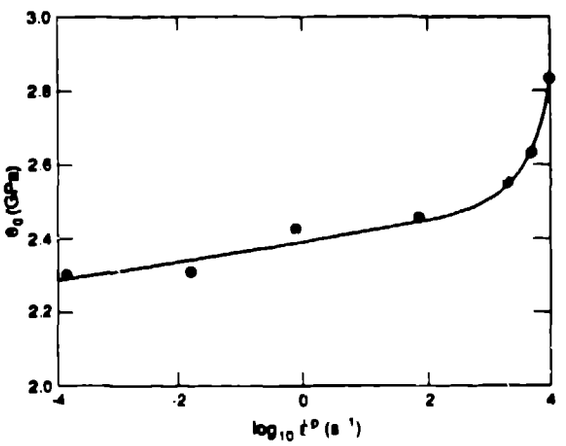

FIGURE 7
Rate-dependent hardening in OFE copper

Follansbee[9] has reinvestigated the influence of dislocation drag on the high-strain-rate response of copper using the MTS model. The average dislocation velocity is given by

$$\bar{v} = L\nu_0(\exp[\Delta G(\tau)/kT] + L\nu_0/v(\tau))^{-1} \quad , \tag{18}$$

where ΔG is given by Equation (16) and $v(\tau)$ is given by Equation (6) plus a Taylor factor. Johnson and Tonks[10] applied Equation (18) to experimental data on shock rise times in copper and concluded (as did Clifton[2] for 6061-T6 aluminum) that the approximately linear dependence of $v(\tau)$ is incapable of representing the rapid increase in strain rate as a function of impact stress. Follansbee[11] has been examining this question in terms of a stress-dependent mobile dislocation density.

2.6. Tonks and Johnson

Tonks and Johnson[7] consider the problem of transition to dislocation drag in terms of the MTS model. Shear stress, plastic strain, and plastic strain rate data are extracted from 3.0- and 5.4-GPa shock waves in OFE copper. This resulted in a new fit to the $\theta(\dot{\epsilon}^P)$ data of Figure 7 as provided by Follansbee:[12]

$$\theta_0(\text{kbar}) = (1/2)[23.707 + 0.08295 \ln \dot{\epsilon}^P(s^{-1}) + 0.03506 \sqrt{\dot{\epsilon}^P(s^{-1})}] \quad . \tag{19}$$

When integrated through the strain-rate history of the 3.0- and 5.4-GPa shock waves, Equation (19) yields final flow stresses consistent with the shock data as well as with the intermediate strain-rate data of Follansbee and Kocks:[6] Figure 8.

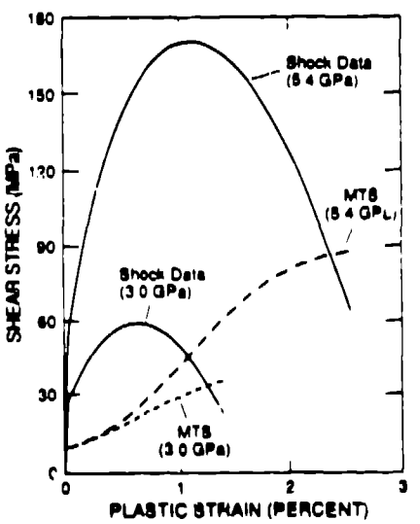

FIGURE 8
Shear stress and MTS evolution in shock compression

3. TRANSITION TO DISLOCATION DRAG IN COPPER

As a means of estimating conditions under which transition from thermal activation to dislocation drag occurs in copper, we note that when the thermal-activation waiting time and the run time between obstacles are additive, as in the development of the models

described here, the plastic strain rate due to both processes occurring simultaneously can be written as

$$\dot{\epsilon}^P = [(1/\dot{\epsilon}_t^P) + (1/\dot{\epsilon}_d^P)]^{-1} \quad . \qquad (20)$$

Here subscripts t and d refer to thermal activation and drag, respectively. Tonks and Johnson[7] observe that the 3.0 - and 5.4-GPa shock-waves are almost entirely in the drag regime. The following is an empirical fit to the 3.0-GPa data [units; s^{-1} and GPa]:

$$\dot{\epsilon}_d^P = 10^d(\tau - h\epsilon^P)^g(\epsilon^P + \epsilon_0^P)^c \quad , \qquad (21)$$

where d = 10.755, h = 1.55 GPa, g = 2.072, ϵ_0^P = 0.0001, and c = 1.09. Thermal activation dominates the deformation process when $\dot{\epsilon}_t^P < \dot{\epsilon}_d^P$ and drag dominates when the inequality sign is reversed. Hence the boundary between the two regions is given by

$$\dot{\epsilon}_t^P = \dot{\epsilon}_d^P \quad , \qquad (22)$$

where $\dot{\epsilon}_d^P$ is given by Equation (21), $\dot{\epsilon}_t^P$ is given by Equation (14), and $\theta_0(\dot{\epsilon}^P)$ is given by Equation (19). This gives the boundary between the thermal activation and dislocation drag regimes as shown in Figure 9 for flow paths at constant plastic strain rate.

The results shown in Figure 9 indicate that dislocation drag is important only at low plastic strains and high plastic strain rates. As the plastic strain rate decreases, it is found that the boundary between the two regimes moves closer to the $\epsilon^P = 0$ axis. Uncertainties in the various functional forms used in the calculation defined by Equation (22) do not allow us to determine whether dislocation drag persists at $\epsilon^P = 0$ and intermediate strain rates ($<10^4 s^{-1}$).

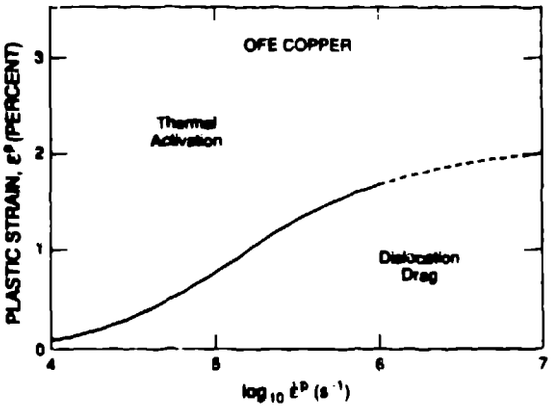

FIGURE 9
Thermal activation and dislocation drag regimes in OFE copper

4. DISCUSSION

We have combined shock-wave data in the form of Equation (21) with intermediate strain-rate data for copper in order to determine the boundary between thermal-activation-dominated and dislocation-drag-dominated plastic flow in OFE copper.

A unique determination of the transition is complicated by the path-dependent nature of the MTS model (above). As pointed out in Section 2.5, OFE copper has a memory of its past history through evolution of τ_a. This problem does not occur for simple rate-dependent (but path-independent) constitutive descriptions: Equation (21) is an example of this type of description. Hardening rules for <u>both</u> thermal activation and viscous drag which depend only on the amount of plastic strain that has been accumulated to that point provide unique interpretation of the transition from thermal activation to viscous drag, but may miss some of the subtler and more interesting aspects of dynamic material behavior.

The question of which type of description is "best" depends on factors such as required accuracy, path variation, and available time resolution. While path-dependent models are

undoubtedly more advanced and more interesting they can also be somewhat more difficult to use.

Tonks[13] has obtained empirical fits to weak-shock data for other solids (Al, Be, Fe, stainless steel, U, and V) using the analysis of Wallace[14]. These data are presented in tabular form with shear stress and plastic strain as functions of time through the shock front. This allows researchers to fit the data with whatever model they think is appropriate. Tonks provides fits to these data in the form of Equation (21).

This collection of weak-shock data can be used to determine transition from thermal activation to dislocation drag in materials other than OFE copper, as intermediate strain-rate data for these materials become available.

REFERENCES

1. D.C. Pack, W.M. Evans, and H.J. James, Proc. Phys. Soc. 60, part 1 (1948) 1.

2. R.J. Clifton, Plastic Waves: Theory and Experiment, in: Shock Waves and the Mechanical Properties of Solids, eds. J. J. Burke and V. Weiss, Syracuse University Press (1971) pp. 73-116.

3. K.G. Hoge and A.K. Mukherjee, J. Mat. Sci. 12 (1977) 1666.

4. P.S. Follansbee, G. Regazzoni, and U.F. Kocks, The Transition to Drag-Controlled Deformation in Copper at High Strain Rates, in: 3rd Conf. Mech. Prop. High Rates of Strain, ed. J. Harding, Institute of Physics Conference Series No. 70, London (1984) pp. 71-80.

5. R.W. Armstrong and F.J. Zerilli, Dislocation Mechanics Based Analysis of Material Dynamics Behavior, Journal de Physique, Colloque C3, Supplément au n_o 9, Tome 49 (1988) pp. 529-534.

6. P.S. Follansbee and U.F. Kocks, Acta Metall. 36 (1988) 81.

7. D.L. Tonks and J.N. Johnson, Shock-Wave Evolution of the Mechanical Threshold Stress in Copper, in: Shock Compression of Condensed Matter - 1989, eds. S. C. Schmidt, J. N. Johnson, and L. W. Davison, Elsevier Science Publishers B.V., Amsterdam (1989) pp. 333-336.

8. D. Steinberg and C.M. Lund, A Constitutive Model for Strain Rates From 10^{-4} to 10^{6} s^{-1}, Journal de Physique, Colloque C3, Supplément au n_o 9, Tome 49 (1988) pp. 433-440.

9. P.S. Follansbee, The Rate Dependence of Structure Evolution in Copper and its Influence on the Stress-Strain Behavior of Copper at Very High Strain Rates, in: Impact Loading and Dynamic Behavior of Materials, eds., C.Y. Chiem, H.-D. Kunze, and L. W. Meyer, Deutsche Gesellshaft für Metallkunde, Vol. 1 (1988) pp. 315-322.

10. J.N. Johnson and D.L. Tonks, Los Alamos National Laboratory Report LA-11993-MS, January 1991.

P.S. Follansbee, personal communication, 1990.

12. P.S. Follansbee, personal communication, 1988.

13. D.L. Tonks, Los Alamos National Laboratory Report LA-12068-MS, May 1991.

14. D.C. Wallace, Phys. Rev. B 22, (1980) 1477 and 1487.